# CONCEPTUAL STUDY FOR AN AUTONOMOUS ROTORCRAFT FOR EXTREME ALTITUDES

A. Barth*, R. Feil**, K. Kondak*** and M. Hajek**

* Munich Aerospace Scholarship Holder, Mail: barth@ht.mw.tum.de, Phone: +49-(0)89-289-16299
** Institute of Helicopter Technology, Technische Universität München (TUM), Boltzmannstr. 15, 85748 Garching, Germany
*** Institute of Robotics and Mechatronics, German Aerospace Centre (DLR), Münchner Strasse 20, 82234 Oberpfaffenhofen, Germany

## ABSTRACT

This paper is devoted to lightweight rotary wing UAVs for applications at extreme high altitudes of up to 9000m, such as search and rescue as well as different types of environmental monitoring. Up to now, such rotary wing UAVs have not been available. Consequently, experience in design and operation of rotary wing UAVs in such environments is lacking. This situation motivates our team from DLR and TUM to work on an all-electric prototype of this kind of rotary wing UAV. The first experimental missions should be performed at altitudes of 5000 to 9000m above sea level. This paper shows the project's current status and preliminary results. We present procedures for preliminary rotor designs and electrical power supplies as well as a tool developed for exploration of the influence of critical design parameters from a mission based point of view. Using the described procedures and the tool, we present the preliminary design of the UAV prototype, which is a synchropter with two counter-rotating and intermeshing rotors. Some of preliminary calculations were verified with flight experiments (hover performance) at different altitudes of up to 5200m above sea level. The results presented, illustrate the feasibility of developing rotary wing UAVs for selected applications at extremely high altitudes and will be the cornerstone for a detailed design of the first prototype.

## NOMENCLATURE

| | |
|---|---|
| $c$ | Rotor blade chord length [m] |
| $C_P$ | Rotorcraft power coefficient [-] |
| $C_T$ | Main rotor(s) thrust coefficient [-] |
| $\eta$ | Efficiency [-] |
| $i$ | Battery current [A] |
| $\kappa$ | Induced power factor [-] |
| $N$ | Rotor rotational speed [min$^{-1}$] |
| $R$ | Rotor blade radius [m] |
| $T_c$ | Battery temperature [°C] |
| $T_a$ | Ambient temperature [°C] |
| $\rho$ | Air density [kg/m$^3$] |
| $V_{tip}$ | Rotor blade tip speed [m/s] |
| $\sigma$ | Rotor solidity [-] |
| $v$ | Battery voltage [V] |
| | |
| AR | Autorotation |
| CS | Cruise speed [m/s] |
| CTR | Conventional tail rotor |
| DLR | German Aerospace Centre |
| FM | Figure of merit [-] |
| GW | Gross weight [kg] |
| HOGE | Hover out of ground effect |
| MIT | Massachusetts Institute of Technology |
| MR | Main rotor |
| MSL | Mean sea level |
| MTOW | Maximum take-off weight [kg] |
| RWUAV | Rotary wing unmanned aerial vehicle |
| ROC | Rate of climb [m/s] |
| TUM | Technische Universität München |

## 1. INTRODUCTION

The evaluation of existing RWUAVs up to MTOW≈25kg (Class 0 [1]) shows that none of them are able to perform missions significantly above 3000m MSL [1] [2]. Expanding the flight envelope would open new fields of applications, such as research in high mountain regions, searches for missed alpinists, or inspection of critical infrastructure (e.g. power supply lines across high mountain ranges). The RWUAV market is growing rapidly. However, while there is much experience available concerning preliminary design of full scale helicopters, there is not much within Class 0, particularly for high altitudes.

It is an interest of the *Munich Aerospace Autonomous Flight* research group *Mission-oriented Design, Control and Equipment* to enrich the experiences and figure out the limits in operating RWUAVs at extreme altitudes up to 9000m MSL. The research group is represented by two partners, *Institute for Robotics and Mechatronics* (DLR) and *Institute of Helicopter Technology* (TUM).

Due to the fact that there is no proper RWUAV available to reach these altitudes, it is necessary to design a new prototype. All-electric power, portable (compact, maximum 25kg), able to operate in harsh mountain regions, off-the-shelf parts, and state of the art battery technology are the major requirements. To achieve these goals, a highly efficient complete system has to be designed. Therefore a

tool has been created that allows the research group to investigate the influence of critical design parameters from a mission based point of view. This paper deals with the first milestone of this project: a preliminary design approach with special focus on rotors and electrical power supply.

## 2. MISSION DEFINITION

The requirement of hovering at 9000m MSL with an MTOW of about 25kg for the prototype, is the mission illustrated in Fig.1 and Tab.1. This mission consists of 6 mission segments, take-off, climbing from 5000 to 9000m MSL, observing for about 2min, autorotation flight state for descending, flying back to base, and landing. The mission should be flown by the autopilot. Due to the constraint of an all-electric drive and state of the art battery technology, the mission's initial altitude is defined at 5000m MSL, the highest altitude that can barely be reached by "normal" human beings.
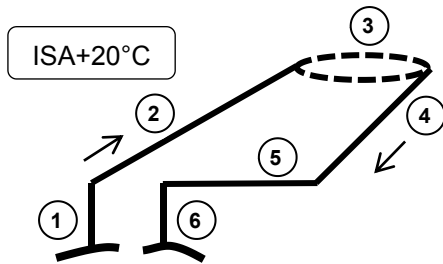


**Fig.1: Mission for a high altitude prototype**

| Mission Segment | Description | Altitude [km] | Time [min] | Speed [m/s] |
|---|---|---|---|---|
| 1 | Take Off | 5 | 2 | 0 |
| 2 | Climb | 5 to 9 | 17 | CS: ≈15 ROC: ≈4 |
| 3 | Observe | 9 | 2 | 0 |
| 4 | Descend | 9 to 5 | 10 | AR |
| 5 | Cruise Inbound | 5 | 8 | CS: ≈15 |
| 6 | Land | 5 | 2 | 0 |

**Tab.1: Mission segment data of the preliminary design mission, corresponding to Fig.1**

## 3. DESIGN APPROACH

### 3.1. Rotor Configuration

The challenge of designing a RWUAV with available batteries and a maximum take-off weight of approximately 25kg demands the complete system to be extremely efficient over the whole mission profile. With regard to the rotor this means low values of blade loading at sea level are necessary, reducing power and retarding the onset of stall at higher altitudes. These low values of blade loading increase the figure of merit at high altitudes.

The selection of the rotor system depends on several criteria:

- Hover and climb efficiency at high altitudes
- Portability (compactness)
- Good autorotation qualities
- Robustness (no tail rotor failure)
- Easy to control (symmetric rotors)
- Use of off-the-shelf parts

Compared to a CTR with same disc loading, dual rotor configurations while hovering or at low speeds generally require less power for a given thrust [3]. Furthermore, coaxial and synchropter configurations offer a huge rotor area in a very compact way (shorter and lighter blades, lighter tail-boom). Considering the above constraints, a synchropter configuration was chosen to be used for the prototype.

Statistical methods [1] often serve as a first basis concept in helicopter preliminary design (see Fig.2). In this case, statistical design approaches will not be able to fulfil the demands of the mission requirements because of a lack of experimental data at the desired mission altitudes.
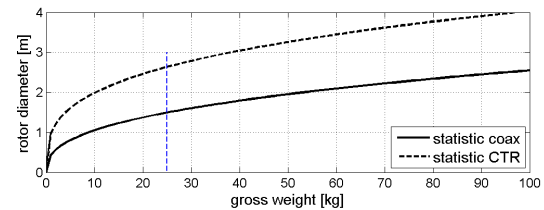


**Fig.2: Statistical rotor sizing presented in [1]**

### 3.2. Description of the Analytical Model

CAMRAD II is an aeromechanics analysis tool for rotorcraft that incorporates a combination of advanced technologies including multi-body dynamics, non-linear finite elements, and rotorcraft aerodynamics [4]. CAMRAD II has been used for the extensive correlation of performance calculations of currently existing flying robots, and for research, development and conceptual design studies for the high altitude flying robot prototype.

As typical for conceptual design studies, low-fidelity models have been used. The rotors are modelled as a set of two rigid blades with 21 aerodynamic panels for each blade. The bearingless blade structure uses teeter joints for blade flapping devices and lag hinges at 121mm radial position.

The aerodynamic model uses two dimensional airfoil tables that were calculated using MSES (by Mark Drela - MIT) to be the most accurate for low Reynolds numbers. The NACA23012 airfoil modified with a tab will be used for analyses shown in this paper and various airfoils will later be examined extensively.

Uniform inflow theory uses, over the range of altitudes, constant induced power correction parame-

ters. The high altitude prototype model – a synchropter configuration – incorporates theoretically approximated constant interference losses [5]. Also, its induced velocity factor for hover was calibrated with a first hover flight test (flown by the type in Fig.5). Lastly, three dimensional airframe polar tables are approximated empirically by resizing data from the Bo105 helicopter.

## 3.3. Battery Model

According to the calculations described in chapter 5 the battery pack contributes more than 1/3 of the helicopter's gross weight for the mission in Tab.1. In order to find a well-balanced preliminary sizing, it is important to estimate battery weight and engine efficiency realistically. The requirements are simply accommodated within a cell simulation model, implemented in Matlab Simulink. The model is based on manufacturers' data sheets and thus can be easily modified for different batteries. There are basically two different types of battery cells:
- High-energy cells
- and high-power cells.

Which type best fulfils the requirements to deliver both- enough energy to complete the mission and enough power for all operating conditions depends on the mission. Due to the relatively long mission time and weight constraints, high energy cells have been chosen to provide most part of the needed energy. For covering power peaks (e.g. controlling gusts), a small high-power pack is envisaged, which is not considered in the following simulation.

Detailed physics based models are generally not suitable for system-level design [6]. Simple dynamic models consisting of capacitor/resistor networks are generally so simplified that they do not represent important phenomena like rate-dependent capacity and temperature effects [6]. Basically the approach described in [6] was used here. Thus, the equilibrium potential is modelled by a procedure using the cell data sheet:
- A typical curve of the cell voltage versus the discharge capacity is approximated using an $n^{th}$-order polynomial
- A rate factor $\alpha(i)$, a temperature factor $\beta(T_c)$, and the temperature and current correction terms $\Delta E(T_c)$ and $\Delta E(i)$ are determined

The temperature and load-dependent cell voltage then can be expressed by

$$(1) \qquad v(i, T_c) = \sum_{k=0}^{n} c_k \cdot (\int_0^t \alpha(i) \cdot \beta(T_c) \cdot i \; dt)^k - \Delta E(T_c) - \Delta E(i).$$

$c_k$ is the coefficient of the $k^{th}$ order term of the polynomial.

The inner heat production of the cell [7] can be described by

$$(2) \qquad P_h = i^2 \cdot R_i + i \cdot U_P + P_{RK}.$$

Hereby the major source of heat is caused by the inner ohmic resistance $R_i$. For the following simulation the polarisation overvoltage $U_P$ and the heat from gas recombination, considered with $P_{RK}$, are ignored. A constant inner cell resistance and a uniform heat distribution are assumed.
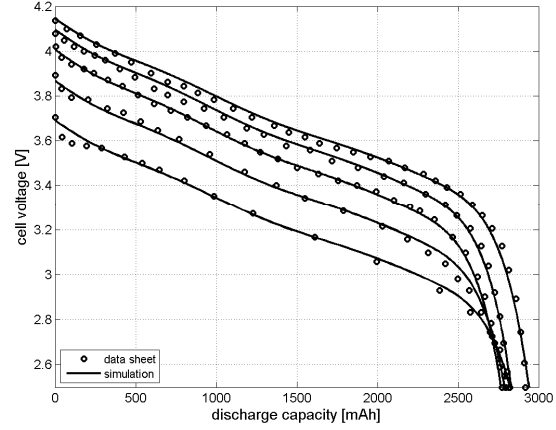


Fig.3: Comparison of the manufacturer's data sheet with the simulation at 25°C (Panasonic NCR 18650PD), from top to bottom: 0.55A, 1.375A, 2.75A, 5.5A and 10A
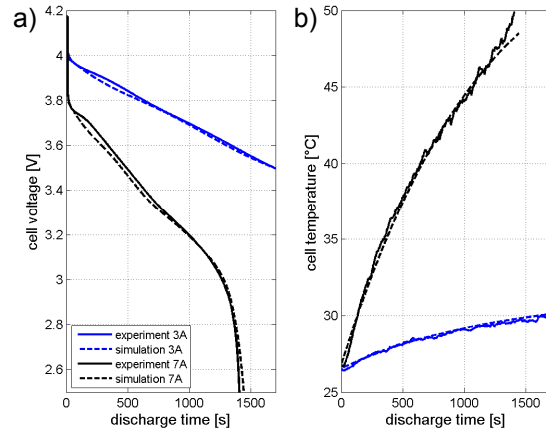


Fig.4: Comparison of constant current (3A, 7A) experiments at constant ambient temperature with the simulation (Panasonic NCR18650PD)

Fig.3 shows that the simulations discharge characteristics at constant temperature agree well with the manufacturer's data. Fig.4 shows that the simulation also agrees well with steady state discharge. This only applies to conditions which are well above the break-off voltage of about 2.5V which has to be avoided to prevent permanent damage. In case of emergency, cells can be discharged to lower voltages to save the prototype. The validation tests were performed by discharging at constant rates of 3A and 7A. In b) the cell temperature is modelled with radiation and convection to approximate the test conditions

$$(3) \qquad T_c = T_c|_{t=0} + \frac{1}{c_c \cdot m_c} \cdot \int_0^t P_{to} dt$$

with the thermal output of the cell

$$(4) \quad P_{to} = i^2 \cdot R_i - c_t \cdot A_c \cdot (T_c - T_a) - \varepsilon_r \cdot \sigma_r \cdot A_c \cdot (T_c^4 - T_a^4).$$

Tab.2 contains the specific model parameters. This model has deficits to represent the transient response during pulsed loads or at the beginning of very high loads, which is mainly caused by diffusion processes inside the cell. This can cause voltage differences at the end of a load spectrum which must considered in the design, for instance by setting the minimal cell voltage to 3V or increasing the number of parallel connected cells. At this time, the thermal model is not able to represent the thermic conditions inside of an insulated battery pack. Hence it is assumed that all cells have an adequate operating temperature ensured by insulation and, if necessary, by heating.

| Name | Symbol | Unit | Value |
|---|---|---|---|
| Cell mass | $m_c$ | $g$ | 45.5 |
| Surface area | $A_c$ | $10^{-3}m^2$ | 3.676 |
| Specific heat | $c_c$ | $\frac{J}{kg\,K}$ | 900 |
| Heat transfer coefficient | $c_t$ | $\frac{W}{m^2K}$ | 3 |
| Radiation heat transfer coefficient | $\varepsilon_r$ | - | 0.95 |
| Stefan-Boltzmann constant | $\sigma_r$ | $10^{-8}\frac{W}{m^2K^4}$ | 5.670 |
| Internal resistance at 3.4V | $R_i$ | $m\Omega$ | 22.88 |

Tab.2: Parameters for the thermal cell simulation (Panasonic NCR18650PD)

### 3.4. Weights and Structures

The current version of the prototype is shown in Fig.5. Hence, the two hubs are located at a fuselage station above the centre of gravity, at a waterline position approximately 350mm above the centre of gravity, and on a sidewise spacing of the buttline position of 138mm for each hub. The opening angle of the two rotor shafts is 24°.

The design study also incorporates iterative procedures on the helicopter's take-off weight, which depends on the chosen design point from which a trim solution for each flight state must be available. The blade mass is approximated to be 6.5kg/m² along its aerodynamic reference area, and therefore depends on its actual radius and chord length. The aircraft basic mass (without blades and battery) used here is assumed to be a constant value of 12.8kg, whereof the avionics with sensors and wiring account for 2.5kg and a high-power cell pack for 0.9kg.

To estimate the weight of the helicopter's battery that provides sufficient energy for the defined mission, a detailed design of an example pack is made. The depiction in Fig.6 has 168 cells and weighs about 9.7kg with cabling, 80mm insulation, and carbon body.
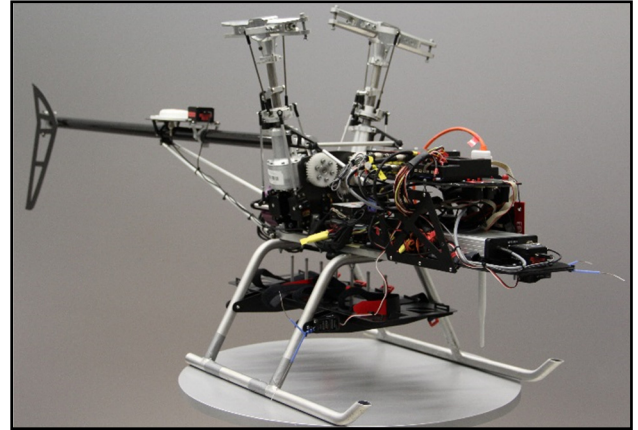


Fig.5: Prototype adduced as a basic model for hover performance and weights
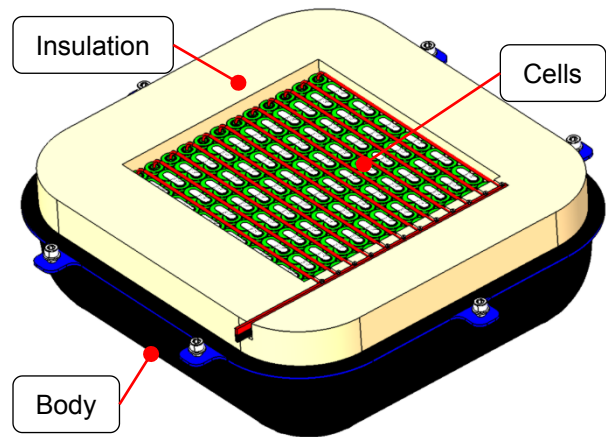


Fig.6: Depiction of a mission battery pack

The cells are arranged in rows of 14 serial connected cells and 12 in parallel. The current drain is carried out by a current bar.

Depending on the actual design configuration and its energy demand, the number of cells in parallel connection of the actual battery pack will be adapted accordingly. The serial number of cells must be held constant in order to comply with the requirements of voltage for the intended engine and current limiting of the used cells.

The process is characterized by the following. The blades weight may increase for a longer radius which can improve aerodynamic efficiencies in high altitudes and therefore reduce the number of cells required. Hence, there are certain limits for blade design, such as maximum aspect ratios for manufacturing issues. Relatively long blades also demand a certain chord length which then increases the blades' weight. Also, in general, lower tip speeds demand less energy, with certain blade designs requiring higher tip speeds in order to be aerodynamically efficient at each stage during the mission. The challenge is to balance the whole system for its two main purposes:

- Aerodynamically efficient for high altitude mission profile

- Take-off weight within Class 0

First studies show that blade twists do not reduce the mission energy significantly. An optimal blade shape will be part of the detailed design of the final prototype.

## 3.5. Model Overall Optimization Procedure

Model consolidation is implemented in Matlab. Pre-defining an n-dimensional array of the rotor design points to be calculated, n is the number of design variables that itself is a vector. The definition of the mission profile, an initializing gross weight of the physical simulation model, and each design point analysis are done independently.
The model integrates the following:
- Physical simulation model of the synchropter (CAMRAD II)
- Automated process for model adaption according to specific design points
- Automated reading procedures of the simulation output
- Battery simulation model (Simulink)
- Gross weight convergence control
- Engine efficiency convergence control

The required rotorcraft power of each mission segment is then determined for a set of design parameters. Gearbox efficiencies are reckoned to be constant and engine efficiencies are initiated using engine tables. Constant gearbox efficiencies are used in order to cover the assumption of constant splashing-, bearing- and tooth friction losses.
Rotor power, gearbox- and engine efficiencies result in the equivalent power that is extracted from the battery.

$$(5) \qquad P_{Battery} = \frac{P_{Rotors}}{\eta_{Gear} \cdot \eta_{Engine}}$$

This power is then used by the battery simulation model to determine its cell characterizing parameters – such as electrical current and voltage – time dependent on the whole mission. An identical load for each cell is implied. Limits for the electrical current and the voltage of the high energy cells must be kept. If not, the number of parallel cells will be adjusted. The determined values for the electrical current are again used to determine the engine efficiencies. This process is being iterated until the values converge to a 1% difference between two iterations.
Once the energy has converged and the corresponding battery is configured, the rotorcrafts' new gross weight is determined. Again an iteration process is used until the gross weight converges within 0.3kg. Once convergence is reached, the results are accumulated and the next design process is started.
This process results in a comprehensive pre-design array for the set of initial conditions of a specific rotorcraft configuration. The process cycle is outlined in Fig.7.
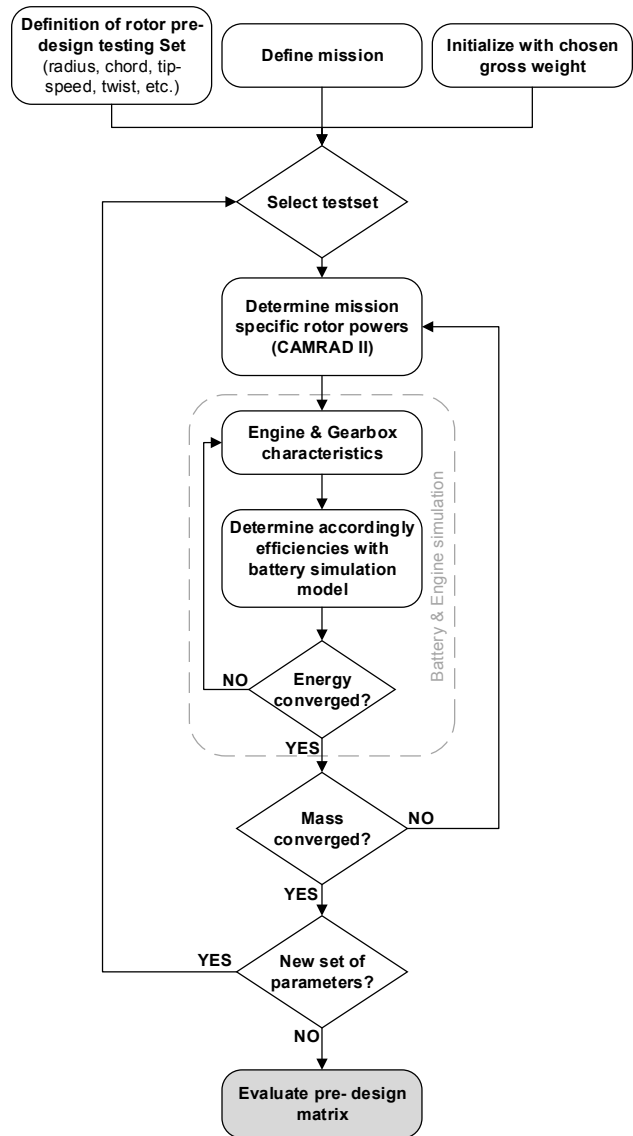


Fig.7: Design process

## 4. VERIFICATION OF ALTITUDE HOVER PERFORMANCE WITH FLIGHT TESTS



**Fig.8: Helicopter (GW about 5kg) modified for high altitude measurements, HOGE at 5170m MSL**

There are two reasons for high altitude flight tests: on the one hand, the gross weight is an important variable in helicopter pre-design. The above mentioned high battery- to gross weight ratio, and the fact that this ratio is constant over the mission time, shows that the battery weight plays a key role and therefore the performance calculation is essential as well. For checking the error margin of a power calculation with low fidelity models over a high altitude range, hover flight tests have been performed with different weights and tip speeds up to 5170m MSL. On the other hand, the design mission (see Tab.1) starts at an altitude of about 5000m MSL. This is a harsh and extreme environment for both human beings and technical equipment to perform flight tests. To be able to undertake a future high altitude prototype flight, it is necessary to gain experience performing such expeditions.

Because of logistical reasons, for these first high altitude test flights a very lightweight and small commercial available helicopter was chosen (see Fig.8). It then was equipped with special electronics for data logging. The numeric values of the settings performed in each altitude can be found in Tab.4.

For comparing the flight test data with CAMRAD II calculations, the main rotor characteristics power coefficient (6), thrust coefficient (7), and figure of merit (8) are calculated by using the measured electrical power $P_{el}$. A total efficiency $\eta_{tot}$ is formed that already contains a constant tail rotor power that quotes 10% of the main rotor power.

$$(6) \qquad C_P = \frac{P_{el} \cdot \eta_{tot}}{\rho \cdot R^2 \pi \cdot V_{tip}^3}$$

$$(7) \qquad C_T = \frac{GW \cdot g}{\rho \cdot R^2 \pi \cdot V_{tip}^2}$$

$$(8) \qquad FM = \frac{\sqrt{C_T^3}}{\sqrt{2} \cdot C_P}$$

The physical model is built up analogously to the model described in 3.1, only using a CTR configuration.
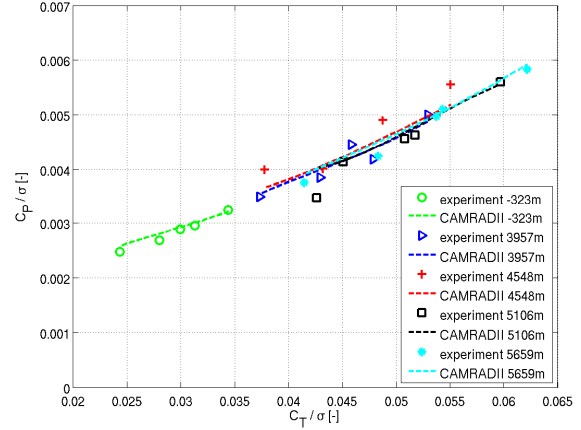


**Fig.9: Comparison of main rotor hover performance with CAMRAD II calculations (legend: density altitude)**
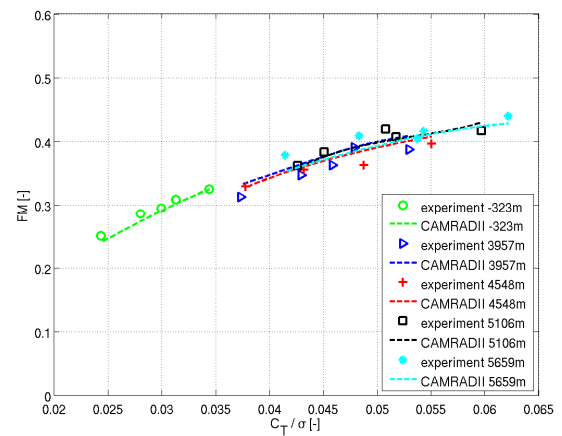


**Fig.10: Comparison of main rotor figure of merit while hovering with CAMRAD II calculations (legend: density altitude)**
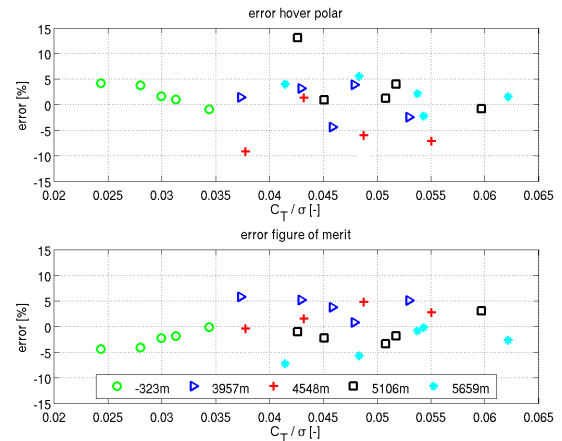


**Fig.11: Difference between experiments and calculations corresponding to Fig.9 and Fig.10 (legend: density altitude)**

The main rotor blade is scanned and 2-D airfoil tables for each altitude are created with MSES. The tail rotor is approximated using a NACA0012 airfoil. The only parameter adjusted is the empirical induced power factor, which is set to 1.2 for Fig.9 and Fig.10. The CAMRAD II solutions are approximated with a 3rd order polynomial. Although a constant induced power factor is used for a density altitude

range of nearly 6000m, the calculation of hover performance and hover figure of merit prediction are possible within a range of ±10% (see Fig.11). This is judged as reasonable for preliminary investigations.

| Name | Symbol | Unit | Value |
|---|---|---|---|
| MR radius | $R$ | $mm$ | 655 |
| MR chord length | $c$ | $mm$ | 55 |
| MR airfoil thickness | - | % | 13.5 |
| MR number of blades | - | - | 2 |
| MR solidity | $\sigma$ | - | 0.0535 |
| Induced power factor | $\kappa$ | - | 1.20 |
| Total efficiency (engine + gearbox) | $\eta_{tot}(i)$ | % | 75.9-77.3 |

**Tab.3: Values used for the calculations in Fig.9 to Fig.11**

| Flight Nb.: | Setting | Values |
|---|---|---|
| 1 | GW$_1$, MR N$_1$ | GW$_1$ = 4.25kg |
| 2 | GW$_1$, MR N$_2$ | GW$_2$ = 4.90kg |
| 3 | GW$_2$, MR N$_1$ | GW$_3$ = 5.55kg |
| 4 | GW$_2$, MR N$_2$ | MR N$_1$ = 1800min$^{-1}$ |
| 5 | GW$_3$, MR N$_2$ | MR N$_2$ = 2000min$^{-1}$ |

**Tab.4: Test set up for collecting the measurements of hover performance at different altitudes**

## 5. PRE- DESIGN ARRAY EVALUATION

The sizing environment as presented in chapter 3 easily allows variations of design and mission parameters. In addition, CAMRAD II can be adapted for a more detailed aero-mechanical model if necessary. Different battery, engine, and gearbox characteristics, as well as adaptions for relaxation and convergence parameters can be implemented. Afterwards, a set of preliminary design configurations can be chosen for detailed investigations. In this case, attention is turned to the configurations that need minimum mission energy at minimum gross weight but still comply with other constraints such as manufacturing aspects, wind vane stability, controllability etc.

Fig.12 shows the partial output of the tool described in chapter 3 for the high altitude prototype. A NACA23012 airfoil, Panasonic 18650B battery and Hacker Q80 engine tables are integrated in the model. The gearbox is simplified with a constant total efficiency of 83% for 3 dry running spur gear stages and 2 worm stages with splash lubrication. Each mission point in Fig.12 consists of 6 free flight operation conditions and has exited the design task described in Fig.7. The blade tip speed varies between 90 and 160m/s, the radius between 1 and 2m, and the chord length between 80 and 140mm. Each point has converged for a gross weight less than 35kg. Higher tip speeds generally consume more power.

Fig.13 exemplary plots the mission energy versus the radius for a constant chord length and tip speeds, whereas Fig.14 plots the mission energy versus the chord length for constant radius and tip speeds. The blade radius does not affect the total mission energy significantly but a larger blade chord consumes higher mission energies. In contrast, looking only at hovering at 9000m, rotor power declines with bigger radii and smaller chord length.

Corresponding to the marked square in Fig.12, the composition of the rotorcraft power with its different amounts of induced, profile, interference, and parasite power is plotted for 5000 and 9000m MSL in Fig.14. As expected, induced power increases with the altitude, but with the profile power dropping at the same time. Interference losses are not seen quantitatively as the interference factors within the simulation model have yet to be validated by conducting further synchropter flight tests.

Fig.16 shows the voltage drop and the corresponding load spectrum of the marked square in Fig.12. Further output of the battery model consists of the cell current and the capacity used over the mission time as well as the number of cells needed and the estimated battery weight.
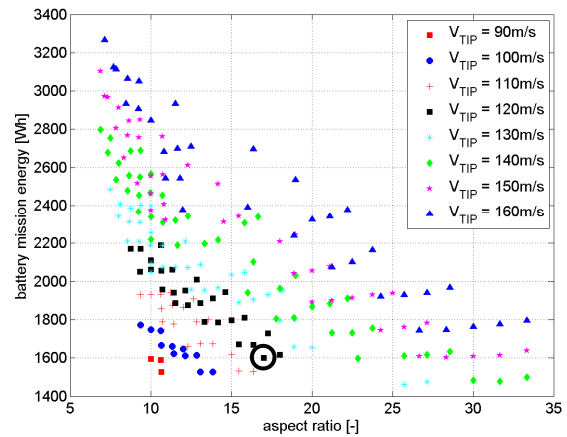


**Fig.12: Results of a variation of R, c and V$_{tip}$ for a synchropter performing the mission shown in Tab.1**
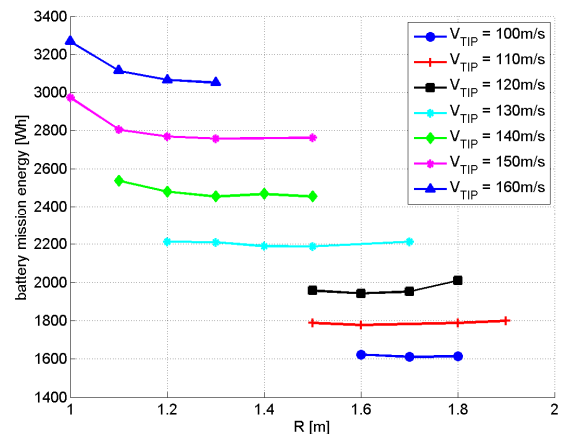


**Fig.13: Radius characteristics for a constant chord length of c=140mm**
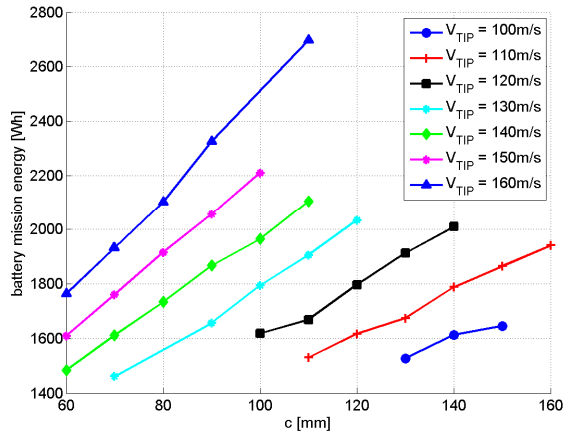
**Fig.14: Chord characteristics for a constant radius of R=1.8m**
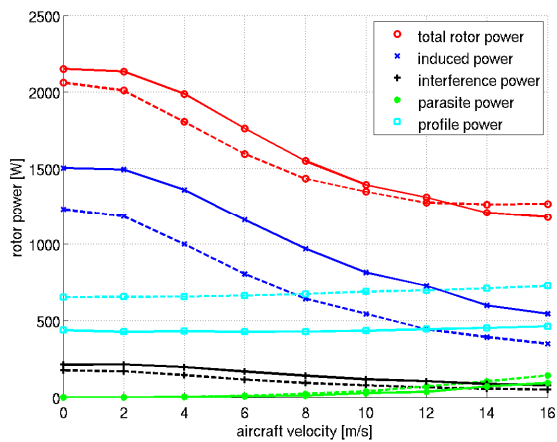


**Fig.15: Sum of rotor power in forward flight. Dashed line: 5000m MSL, solid line: 9000m MSL. GW=27kg, R=1.7m, c=100mm and $V_{tip}$=120m/s (see marked square in Fig.12).**
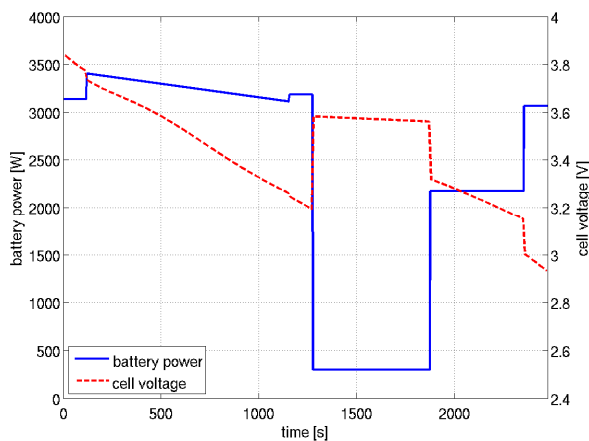


**Fig.16: Example of the mission power of the battery and the cell voltage of a single Pansonic 18650B cell within the battery pack (14 serial, 12 parallel). GW=27kg, R=1.7m, c=100mm and $V_{tip}$=120m/s (see marked square in Fig.12).**

## 6.  CONCLUSION

The first year's assignment was to deliver a preliminary conceptual study for the requirement to hover at 9000m MSL with a full-electric Class 0 RWUAV. Therefore a mission was defined, analysed and accordingly a synchropter rotor configuration for this intent was chosen. A sizing environment using CAMRAD II and Matlab was created that is able to predict both rotor and battery performance during the whole mission time in a sufficient way for pre-design. The tool is used for the specific case of a high altitude prototype but has the flexibility to embed different engine and battery types, missions, and rotor configurations. The influence of important rotor design parameters such as tip speed, radius and chord length have been investigated extensively for a high altitude mission. Thereby the foundation was laid for a detailed design. E.g.: A configuration with R=1.7m, c=100mm and $V_{tip}$=120m/s converges for a gross weight of 27kg and requires a battery pack with 168 Li-ion cells (Panasonic 18650B) for the mission energy of 1601Wh.

An expedition was made up to 5200m MSL whereupon valuable experience was obtained camping and doing field experiments in high altitude mountain regions. It was shown that low-fidelity models can predict hover performance sufficiently for preliminary design studies over a range of altitudes.

Ongoing work includes the development of a very lightweight, robust carbon/glass fibre rotor blade based on a design choice that was made using the tool presented in this paper. For stepwise validation of the CAMRAD II model, component tests as well as more high altitude flight tests with a scale synchropter (GW≈17kg) will be performed. In parallel, the development of an autopilot with a special focus on very low blade loadings at low air density will be initiated.

## REFERENCES

[1] Khromov V., Rand O.: *Design Trends for Rotary-Wing Unmanned Air Vehicles*, 25th International Congress of the Aeronautical Sciences, Germany, 2006

[2] *Unmanned Vehicles*, Issue 22, The Shephard Press Ltd, England, 2014

[3] Colin P. Coleman: *A Survey of Theoretical and Experimental Coaxial Rotor Aerodynamic Research*, NASA Technical Paper 3675, Ames Research Center, Moffett Field, California, 1997

[4] Johnson W.: *Technology Drivers in the Development of CAMRAD II,* American Helicopter Society Aeromechanics Specialists Conference, San Francisco, California, January 19-21, 1994

[5] Leishman J.G.: *Principles of Helicopter Aerodynamics.* Cambridge University Press, New York 2006

[6] Gao L., Liu S., Dougal R.A.: *Dynamic Lithium-Ion Battery Model for System Simulation.* EEE Transactions on Components and Packaging Technologies, 3. September 2002, Vol. 25

[7] Jossen A., Weydanz W.: *Interne Wärmequellen und -senken. Moderne Akkumulatoren richtig einsetzen.* München und Leipheim: Inge Reichardt Verlag, 2006

## COPYRIGHT STATEMENT